Drift Surfaces in Linear and Axisymmetric Magnetic Fields

J.E. Howard

June 1976

UWFDM-163

FUSION TECHNOLOGY INSTITUTE

UNIVERSITY OF WISCONSIN

MADISON WISCONSIN

Drift Surfaces in Linear and Axisymmetric Magnetic Fields

J.E. Howard

Fusion Technology Institute
University of Wisconsin
1500 Engineering Drive
Madison, WI 53706

http://fti.neep.wisc.edu

June 1976

UWFDM-163

DRIFT SURFACES IN LINEAR AND AXISYMMETRIC MAGNETIC FIELDS

JAMES E. HOWARD

JUNE 1976

UWFDM-163
(revised May 1978)

FUSION TECHNOLOGY PROGRAM

NUCLEAR ENGINEERING DEPARTMENT

UNIVERSITY OF WISCONSIN

MADISON, WISCONSIN 53706

"LEGAL NOTICE"

"This work was prepared by the University of Wisconsin as an account of work sponsored by the Electric Power Research Institute, Inc. ("EPRI"). Neither EPRI, members of EPRI, the University of Wisconsin, nor any person acting on behalf of either:

"a. Makes any warranty or representation, express or implied, with respect to the accuracy, completeness, or usefulness of the information contained in this report, or that the use of any information, apparatus, method, or process disclosed in this report may not infringe privately owned rights; or

"b. Assumes any liabilities with respect to the use of, or for damages resulting from the use of, any information, apparatus, method or process disclosed in this report."

DRIFT SURFACES IN LINEAR AND AXISYMMETRIC MAGNETIC FIELDS

James E. Howard

Nuclear Engineering Department
University of Wisconsin
Madison, Wisconsin 53706

ABSTRACT

Banana orbits are calculated for linear and axisymmetric magnetic fields with axial currents by an approximate integration of the drift equations. Excellent agreement is demonstrated with computed drift surfaces for a stuffed quadrupole cusp.

1. INTRODUCTION

Trapped particles play an important role in transport processes in tokamak fields (GALEEV and SAGDEEV, 1968; KADOMTSEV and POGUTSE, 1971), and much theoretical effort has been expended in determining their properties (ARTSIMOVICH, 1972; FURTH, 1975). Under adiabatic conditions, the poloidal projection of trapped particle orbits form closed curves, the so-called "bananas", whose width is a key parameter in neoclassical diffusion. Previous treatments of banana orbits have been limited to tokamak fields.

In this paper we study drift surfaces in an arbitrary linear two dimensional static magnetic field with an added constant B_z, and an arbitrary poloidal field with an added $B_T \sim 1/R$. Axial currents are allowed in both cases. The banana width is derived directly from the drift equations in the small-width limit, and compared with a more general expression including finite gyroradius terms, obtained from the constancy of p_z in the linear case, and p_ϕ in the axisymmetric case. A useful correction factor is derived for large widths via the guiding center equations. These expressions may be applied to any low-β axisymmetric plasma device without poloidal currents, such as tokamaks or toroidal multipoles. Detailed comparison is made with computed orbits and drift surfaces in a stuffed quadrupole cusp.

2. TWO-DIMENSIONAL FIELD WITH AN ADDED CONSTANT B_z

Consider particle motion in the field depicted in Fig. 1. The two dimensional ("poloidal") part of the field is assumed derivable from a stream function ψ according to

$$\underline{B}_p = \hat{\underline{z}} \times \nabla\psi \ . \qquad (1)$$

Writing $\underset{\sim}{B} = \underset{\sim}{B}_p + \underset{\sim}{B}_z$ where B_z may be an arbitrary function of space, we have $\underset{\sim}{B}_p \cdot \nabla\psi = \underset{\sim}{B} \cdot \nabla\psi = 0$. Thus, the total field lies in the flux surface ψ = constant. $\nabla \cdot \underset{\sim}{B} = 0$ then requires B_z to be independent of z, while $\nabla \times \underset{\sim}{B} = \frac{4\pi}{c} \underset{\sim}{J}_z$ implies independence of x and y. Therefore, B_z = constant and p_z is conserved. In order to have closed drift surfaces, we assume that the field possesses a symmetry plane where B reaches a local minimum.

The drift velocity is (SCHMIDT, 1966)

$$\underset{\sim}{v}_D = v_{\parallel} \hat{\underset{\sim}{s}} + \frac{\varepsilon}{2B^3} (2v^2 - \mu B) \underset{\sim}{B} \times \nabla B + \frac{4\pi\varepsilon v_{\parallel}^2}{cB^2} \underset{\sim}{J}_{\perp} , \tag{2}$$

where $\hat{\underset{\sim}{s}} = \underset{\sim}{B}/B$, $\varepsilon = mc/e$ and $\mu = v_{\perp}^2/B$ is the magnetic moment, assumed strictly constant. $\underset{\sim}{J}_{\perp}$ clearly makes no contribution to the banana width and will be set equal to zero in what follows. Expressing ∇B in poloidal coordinates we have

$$\underset{\sim}{B} \times \nabla B = \frac{B_p^3}{B} \kappa \hat{\underset{\sim}{z}} - \frac{B_z B_p^2}{B} \kappa' \hat{\underset{\sim}{n}} - \frac{B_z B_p^2}{B} \kappa \hat{\underset{\sim}{\ell}} , \tag{3}$$

where $\hat{\underset{\sim}{\ell}} = \underset{\sim}{B}_p/B_p$, $\hat{\underset{\sim}{n}}$ is the poloidal normal, chosen such that $\hat{\underset{\sim}{\ell}} \times \hat{\underset{\sim}{n}} = \hat{\underset{\sim}{z}}$, and the poloidal curvatures are given by

$$\kappa = \frac{1}{B_p} \frac{\partial B_p}{\partial n} , \tag{4}$$

$$\kappa' = -\frac{1}{B_p} \frac{\partial B_p}{\partial \ell} . \tag{5}$$

We are interested in the normal component of $\underset{\sim}{v}_D$, that gives the projected drift surface its banana-like appearance;

$$v_{D_n} = \frac{-\varepsilon B_z B_p^2 \kappa'}{2B^4} (2v^2 - \mu B) . \tag{6}$$

Drift surfaces may be rigorously traced out by integrating the differential equations (2). However, we may obtain an approximate expression for the banana width by integrating equation (6) over time, holding ψ constant in the integrand;

$$\Delta n = \int_o^T v_{D_n} \, dt , \tag{7}$$

where T is the bounce period and t = 0 at the midplane. In stream function units,

$$\Delta\psi = \int_0^T \underset{\sim}{v}\cdot\nabla\psi \, dt = \int B_p v_{D_n} dt. \tag{8}$$

Substituting

$$dt = \frac{ds}{v_{//}} = \frac{B d\ell}{B_p v_{//}}, \tag{9}$$

we obtain

$$\Delta\psi = \varepsilon B_z \int_0^{\ell_{max}} \frac{2v^2 - \mu B}{B^3} B_p \frac{\partial B_p}{\partial \ell} \frac{d\ell}{v_{//}}, \tag{10}$$

with ℓ measured from the symmetry plane. This integral may be simplified by observing that

$$dB_p = \frac{\partial B_p}{\partial \ell} d\ell \tag{11}$$

along a field line. Further noting that $B_p \, dB_p = B \, dB$ we obtain

$$\Delta\psi = \varepsilon B_z \int_{B_o}^{B_{max}} \frac{2v^2 - \mu B}{\sqrt{v^2 - \mu B}} \frac{dB}{B^2}, \tag{12}$$

where B_o is the minimum value of B, assumed to occur at the midplane. The corresponding integral for Δn does not seem to be tractable and will not be pursued here.

The integral in equation (12) may now be carried out by taking $x = B/B_{max}$ as variable of integration, noting that $\mu = v^2/B_{max}$. This gives

$$\Delta\psi = \frac{\varepsilon v B_z}{B_{max}} \int_{1/M}^{1} \frac{2 - x}{x^2\sqrt{1-x}} dx, \tag{13}$$

where

$$M = B_{max}/B_o \tag{14}$$

is the <u>orbital</u> mirror ratio. Finally,

$$\Delta\psi = 2\varepsilon v \sqrt{\frac{M-1}{M}} \sqrt{\frac{\gamma}{\gamma+1}} , \tag{15}$$

where

$$\gamma = (B_z/B_{p_o})^2 \tag{16}$$

measures the strength of B_z.

Equation (15) expresses the banana width in stream function units for an arbitrary two-and-a-half dimensional field. Note that $\Delta\psi$ is proportional to the total velocity, proportional to B_z for small B_z, and independent of B_z as $B_z \to \infty$, with B_{p_o} held fixed. Also note that $\Delta\psi$ is proportional to $\sqrt{M-1}$ for small mirror ratios and independent of M for large M.

The banana width may be obtained more simply from the conservation of the z-component of angular momentum as follows:

$$p_z = mv_z + \frac{e}{c}\psi(x,y) \tag{17}$$

is strictly constant along the orbit. To relate this to the guiding center motion resolve v_z along $\underset{\sim}{v}_\perp$ and $\underset{\sim}{v}_{//}$;

$$v_z = \frac{B_z}{B} v_{//} + \frac{B_p}{B} (\hat{\underset{\sim}{\rho}}\cdot\hat{\underset{\sim}{n}}) v_\perp , \tag{18}$$

where $\hat{\underset{\sim}{\rho}}$ is a unit vector along the local gyroradius.

Therefore,

$$\psi + \varepsilon v_{//} \frac{B_z}{B} + B_p \rho_n = \text{constant} \tag{19}$$

where $\rho_n = \underset{\sim}{\rho}\cdot\hat{\underset{\sim}{n}}$ is the projected gyroradius. The width is then given implicitly by

$$\Delta\psi = \psi_2 - \psi_1 = \varepsilon B_z \left(\frac{v_{//1}}{B_1} + \frac{|v_{//2}|}{B_2}\right) + B_{p_1}\rho_1 - B_{p_2}\rho_2 , \tag{20}$$

where the subscripts 1 and 2 denote the points where the two branches of the banana cross the midplane. Equations (19) and (20) are exact.
Under adiabatic conditions,

$$\Delta\psi \simeq \frac{\varepsilon B_z v_{//1}}{B_1} \left[1 + \frac{B_1}{B_2}\left(\frac{M - B_2/B_1}{M-1}\right)^{1/2}\right] + B_{p_1}\rho_{n_1} - B_{p_2}\rho_{n_2} . \tag{21}$$

Note that B_2 need not be close to B_1. Given $B = B(\psi)$ on the median plane and neglecting ρ_1 and ρ_2, equation (21) may be solved implicitly for $\Delta\psi$. As we shall see, the branch correction (in brackets) makes an important contribution for large widths. When the width is small (B_z or M not too large), we may take $B_1 \tilde{\simeq} B_2$ and write

$$\Delta\psi \tilde{\simeq} \frac{2\varepsilon B_z v_{\parallel_o}}{B_o} + B_{p_o} (\rho_{n_1} - \rho_{n_2}) , \tag{22}$$

clearly displaying the separate contributions of the guiding center and finite gyroradius. The first term in equation (22) is easily seen to be equivalent to the right hand side of equation (15). From equation (22) we obtain a condition for the guiding center width to exceed the projected gyrodiameter at the midplane,

$$B_z\sqrt{M-1} > B_{p_o} . \tag{23}$$

When this condition is fulfilled the banana splits into two distinct branches.

To obtain the width in physical units, one might try a Taylor expansion about the initial point:

$$\Delta n \tilde{\simeq} \left(\frac{\partial n}{\partial \psi}\right)_o \Delta\psi = \Delta\psi/B_{p_o} . \tag{24}$$

However, in practice it turns out to be much more accurate to express r as a function of ψ on the midplane and use

$$\Delta n = \Delta r = r(\psi + \Delta\psi) - r(\psi) . \tag{25}$$

3. THE STUFFED QUADRUPOLE CUSP

Figure 2 depicts one quadrant of this minimum-B field. The two dimensional part of the field is

$$\underset{\sim}{B}_p = x\,\hat{\underset{\sim}{x}} - y\,\hat{\underset{\sim}{y}} , \tag{26}$$

derivable from the scalar potential

$$\Phi = \frac{1}{2}(x^2 - y^2) \tag{27}$$

whose harmonic conjugate is the stream function

$$\psi = xy . \tag{28}$$

The total field is then

$$B^2 = x^2 + y^2 + B_z^2 \quad . \tag{29}$$

Note that both B_p and B reach a minimum on the median plane x = y, where $\partial B_p/\partial \ell$ vanishes. Since $\psi = r^2/2$ on the midplane we have a simple expression for the banana width in physical units,

$$\Delta n = \sqrt{2(\psi + \Delta\psi)} - \sqrt{2\psi} \quad , \tag{30}$$

with $\Delta\psi$ given by equation (15). For small $\Delta\psi$,

$$\Delta n \approx \frac{\Delta\psi}{\sqrt{2\psi}} \quad . \tag{31}$$

Both particle orbits and drift surfaces were computed for a stuffed cusp in order to verify equations (15), (24) and (25) for $\Delta\psi$ and Δn. The orbits were needed to investigate finite gyroradius effects and to determine adiabaticity limits, while drift surfaces were easier to analyze for accurate comparisons with theory. Orbits were started at the midplane in the usual way (HOWARD, 1971) with the pitch angle given by $\csc\chi=\sqrt{M}$ and the phase angle chosen for maximum $\Delta\mu$. Time was scaled by taking $\varepsilon = 1$. Figure 3 shows a typical orbit, for the parameters $\psi_o = 1$, M = 2, v = 2, and $B_z = 5$ ($B_z/B_{p_o} = 3.54$). Figure 4 illustrates the special case given by equation (23) where the two branches of the banana just overlap so that the <u>total</u> width is twice the guiding center width.

Figure 5 shows a family of computed drift surfaces for the case M = 1.5, $B_z = 1$ and varying velocity. As v approaches the value v* = 4.5 from below, a limiting curve is approached asymptotically; when v = v* exactly, the surface degenerates to the point $x_o = y_o = 1$; and when v > v* the drift velocity reverses sign, producing the dashed curve shown in Fig. 6. However, orbital studies show that for these parameters adiabaticity breaks down for $v \gtrsim 0.5$, so that the behavior of the drift curves in Fig. 6 is not reflected in actual particle orbits.

Theoretical and computed guiding center widths are compared in Fig. 7 for M = 2, with $\Delta\psi$ calculated iteratively from equation (21) and used in equation (30) to generate Δn. The results are essentially identical. Also shown as the dashed curves are the conventional (uncorrected) widths as given by equation (15) or (22). Without the branch connection sizable errors can occur at higher velocities. For example, when $B_z = 1$ and v = 4, the error is

31%, whereas the corrected width is accurate to four significant figures. Figure 8 compares the two approximations for Δn with the exact width computed from the drift equations as a function of velocity. The full expression (30) is identical to the drift data, while the linearization (31) is almost a factor of two too large at $v = 4$. This figure also illustrates the important fact that $\Delta\psi$ is much more linear in velocity than is Δn.

4. NONADIABATIC DRIFT

In addition to the banana drift, which is strictly accurate only under adiabatic conditions, there is the possibility of a nonadiabatic "drift". This would take the form of a jump in ψ as the orbit crosses the midplane, similar to nonadiabatic jumps in the magnetic moment. After the jump, the orbit would fall on a new drift surface, depending primarily on the gyration phase at the midplane. For the poloidal field alone the nonadiabatic drift is

$$\Delta\psi = \int_{-t}^{t} \underset{\sim}{v}\cdot\nabla\psi \, dt = \int_{-s}^{s} v_n B_p \frac{ds}{v_{||}} \tag{32}$$

or

$$\Delta\psi = \mathrm{Re}\ \sqrt{M} \int_{-\Phi}^{\Phi} \sqrt{B_p} \quad \frac{e^{i\phi} d\Phi}{v_{||}} ,$$

where Φ is the scalar potential and ϕ is the gyration phase. Carrying out the integration for the cusp with $B_z = 0$ as a worst case, we find

$$\frac{\Delta\psi}{\psi} = \frac{2^{1/8}\pi}{4\Gamma(7/8)} \frac{\lambda^{9/8}}{\sqrt{M}} e^{-\alpha/\lambda} \cos\phi_o , \tag{33}$$

where

$$\lambda \equiv \varepsilon v/\psi , \tag{34}$$

and

$$\alpha = \int_{0}^{\pi/2} (1 - M^{-1}\cos^{1/2}\theta)^{-1/2} \cos\theta d\theta . \tag{35}$$

The calculation for nonzero B_z is more complicated and will be reported elsewhere as part of a general study of $\Delta\mu$ for 3-D fields.

To estimate the magnitude of $\Delta\psi$, let us compare it with the corresponding jump in the magnetic moment (HOWARD, 1971),

$$\frac{\Delta\mu}{\mu} = \frac{-\pi}{2^{1/8}\Gamma(9/8)} \frac{\sqrt{M}}{\lambda^{1/8}} e^{-\alpha/\lambda} \cos\phi_o . \tag{36}$$

Thus,

$$\frac{\Delta\psi}{\psi} = \frac{-2^{1/4}\Gamma(9/8)}{4\Gamma(7/8)} \frac{\lambda^{5/4}}{M} \left(\frac{\Delta\mu}{\mu}\right) . \tag{37}$$

Since λ is normally small for slightly nonadiabatic orbits ($\Delta\mu/\mu \lesssim 20\%$), $\Delta\psi/\psi$ will be proportionally smaller than $\Delta\mu/\mu$. As a worst case, taking $M = 2$ and $\lambda = 1$ gives $\Delta\mu/\mu \approx 1$ and $\Delta\psi/\psi \approx 0.15$. These results can be generalized to a wide class of 2-D fields. It should be noted too, that the constancy of $p_z = mv_z + \psi$ prohibits arbitrarily large $\Delta\psi$. We conclude that nonadiabatic cross-field drift makes negligible contribution to particle transport in 2-D fields. Although the full 3-D calculation has not yet been carried out, it seems likely that nonadiabatic drift will prove negligible there also.

The original motivation for this study was to see if a particle would stick to a field line during nonadiabatic motion, which is always most pronounced near the midplane. Since v_D vanishes at a symmetry plane, we are assured that the particle will cling to the field line long enough to identify $\Delta\mu$ with a well defined value of ψ. On the other hand, because of the exponential dependence of $\Delta\mu$ on ψ, it is possible for a drift surface to have an adiabatic outer branch and a relatively nonadiabatic inner branch.

5. AXISYMMETRIC FIELDS

Consider a particle gyrating in an axisymmetric field, as depicted in Fig. 9 The total drift velocity in an arbitrary axisymmetric magnetostatic field, including a toroidal current, is

$$\underset{\sim}{v}_D = v_{\parallel}\hat{\underset{\sim}{s}} + \frac{\varepsilon}{4B^4}(2v^2 - \mu B)(\underset{\sim}{B}_T + \underset{\sim}{B}_p) \times \nabla(B_T^2 + B_p^2) + \frac{4\pi\varepsilon v_{\parallel}^2}{cB^2}\underset{\sim}{J}_{\perp} . \tag{38}$$

The only terms contributing to the poloidal drift are

$$\underset{\sim}{v}_D' = \frac{\varepsilon}{2B^4}(2v^2 - \mu B)\underset{\sim}{B}_T \times (B_T\nabla B_T + B_p\nabla B_p). \tag{39}$$

Putting

$$B_T = C/R, \tag{40}$$

we have

$$\underset{\sim}{B}_T \times \nabla B_T = \frac{B_T^2}{R} \hat{\underset{\sim}{z}} \tag{41}$$

$$\underset{\sim}{B}_T \times \nabla B_p = B_T \frac{\partial B_p}{\partial \ell} \hat{\underset{\sim}{n}} - B_T \frac{\partial B_p}{\partial n} \hat{\underset{\sim}{\ell}}. \tag{42}$$

Thus,

$$v_{D_n} = \frac{\varepsilon}{2B^4} (2v^2 - \mu B) \left[\frac{B_T^3}{R} (\hat{\underset{\sim}{z}} \cdot \hat{\underset{\sim}{n}}) + B_p B_T \frac{\partial B_p}{\partial \ell}\right]. \tag{43}$$

But $\hat{\underset{\sim}{z}} \cdot \hat{\underset{\sim}{n}} = -B_R/B_p$, so that

$$v_{D_n} = \frac{\varepsilon}{2B^4} (2v^2 - \mu B) B_p B_T \left[\frac{\partial B_p}{\partial \ell} - \left(\frac{B_T}{B_p}\right)^2 \frac{B_R}{R}\right] . \tag{44}$$

The first term in brackets dominates in current multipole experiments (LENCIONI, et al., 1968) where B_T is small, while the second dominates in tokamaks. Note that both B_R and $\partial B_p/\partial \ell$ vanish on the median plane. Now in axisymmetric geometry a stream function ψ exists such that

$$B_p = \frac{1}{R} \frac{\partial \psi}{\partial n} , \tag{45}$$

so that

$$\Delta\psi = \int R B_p v_{D_n} \frac{ds}{v_{//}} . \tag{46}$$

Inserting the first term of equation (44) into equation (46), we find

$$\Delta\psi_1 = \varepsilon C \int_{B_{p_o}}^{B_{p_{max}}} (2v^2 - \mu B) \frac{B_p dB_p}{v_{//} B^3} . \tag{47}$$

The second term in equation (44) is best treated by using $ds = BdR/B_R$ and then $B_T\, dR = -R\, dB_T$, giving

$$\Delta\psi_2 = \varepsilon C \int_{B_{T_o}}^{B_{T_{max}}} (2v^2 - \mu B) \frac{B_T dB_T}{v_{//} B^3} . \tag{48}$$

Combining equations (47) and (48) we have

$$\Delta\psi = \varepsilon C \int_{B_o}^{B_{max}} \frac{2v^2 - \mu B}{\sqrt{v^2 - \mu B}} \frac{dB}{B^2} , \tag{49}$$

with exactly the same integral as for the linear case. Thus, writing $C = R_o B_{T_o}$,

$$\frac{\Delta\Psi}{R_o} = 2\varepsilon v \sqrt{\frac{M-1}{M}} \sqrt{\frac{\gamma}{\gamma+1}} , \tag{50}$$

with $\gamma \equiv B_{T_o}^2 / B_{p_o}^2$, in complete analogy to equation (15) for the linear case. This expression is entirely general, applying to tokamaks as well as toroidal multipoles, so long as a symmetry plane exists.* Similar derivations in the Russian literature depend on the specific properties of the tokamak field.

Equation (50) may also be obtained from the conservation of the ϕ component of angular momentum as follows:

$$p_\phi = mRv_\phi + \frac{e}{c}\psi(R,z) \tag{51}$$

is strictly constant along the orbit. Writing

$$v_\phi = \frac{B_T}{B} v_{||} + \frac{B_p}{B}(\hat{\rho}\cdot\hat{n})v_\perp , \tag{52}$$

we have

$$\psi + \frac{\varepsilon C}{B} v_{||} + RB_p\rho_n = \text{const.} \tag{53}$$

Thus,

$$\Delta\psi = \varepsilon C \left(\frac{v_{||1}}{B_1} + \frac{|v_{||2}|}{B_2}\right) + R_1 B_{p_1} \rho_{n_1} - R_2 B_{p_2} \rho_{n_2} . \tag{54}$$

Under adiabatic conditions,

$$\Delta\psi \simeq \frac{\varepsilon C v_{||}}{B_1} \left[1 + \frac{B_1}{B_2}\left(\frac{M - B_2/B_1}{M-1}\right)^{1/2}\right] + R_1 B_{p_1} \rho_{n_1} - R_2 B_{p_2} \rho_{n_2} , \tag{55}$$

which may be solved implicitly for $\Delta\psi$. The banana width exceeds the projected gyrodiameter when

$$B_{T_o}\sqrt{M-1} > B_{p_o} .$$

---

* An interesting exception is the spindle cusp, in which the poloidal field lines do not cross the median plane.

For small widths,

$$\frac{\Delta\psi}{R_o} \simeq \frac{2\varepsilon B_{T_o} v_{\parallel_o}}{B_o} + B_{p_o} (\rho_{n_1} - \rho_{n_2}) \ . \qquad (57)$$

The first term is readily seen to be equivalent to the guiding center expression (50), again establishing formal correspondence between the two approaches. As in the linear case, it is well worth the trouble to invert $\psi = \psi(R)$ to obtain an accurate value of the width in physical units. The first term of equation (55) should be solved iteratively for $\Delta\psi$ for toroidal multipoles having small B_T/B_p, while equation (50) can be used directly for tokamaks. Finally, we note that the first term of equation (57) may be combined with equation (45) to obtain

$$\Delta n \cong 2\rho_o A \sqrt{M-1}, \qquad (58)$$

where $A \equiv B_{T_o}/B_{p_o}$ is the aspect ratio and ρ_o is the gyroradius at the midplane.

ACKNOWLEDGEMENTS

This research was supported by the Electric Power Research Institute.

The author would like to thank Prof. G. A. Emmert and Dr. H.R. Lewis for several helpful discussions.

FIGURE CAPTIONS

Fig. 1. Two-dimensional field with an added B_z. The total field has a local minimum on the midplane.

Fig. 2. Stuffed quadrupole cusp. The field lines lie in hyperboloidal sheets $\Psi = xy$.

Fig. 3. Banana orbit in quadrupole cusp, with $\Psi_o = 1$, $M = 2$, $B_z = 5$, and $v = 2$.

Fig. 4. No-overlap case, with $M = 2$, $B_z = 1.6$, and $v = 0.5$. The total width is twice the guiding center width.

Fig. 5. Drift surfaces in quadrupole cusp, starting from the point $x = y = 1$, with $M = 1.5$ and $B_z = 1$.

Fig. 6. Limiting drift surface as $v \to 4.50$. When $v = 4.50$ exactly the line $x = y$ occurs and when $v > 4.50$ the drift reverses, producing the dashed curve. Since adiabaticity is violated, actual particle orbits do not follow these curves.

Fig. 7. Banana width as a function of B_z for the quadrupole cusp. The dots were taken from computed drift surfaces and the curves represent the analytical formulas.

Fig. 8. Banana width as a function of v. The solid curve is from equation (30), the dashed curve is the linearized expression, and the dots are computed valves.

Fig. 9. Axisymmetric field geometry.

REFERENCES

ARTSIMOVICH, L. A. (1972) Nucl. Fusion 12, 215.

FURTH, H. P. (1975) Nucl. Fusion 15, 487.

GALEEV, A. A. and SAGDEEV, R. Z. (1968) JETP 26, 233.

HOWARD, J. E. (1971) Physics Fluids 14, 2378

KADOMTSEV, B. B. and POGUTSE, O. P. (1971) Nucl. Fusion 11, 67.

KRUSKAL, M. D. and Kulsrud, R. M. (1958) Physics Fluids 1, 265.

LENCIONI, D. E., POUKEY, J. W., SCHMIDT, J. A., SPROTT, J. C. and ERICKSON, C. W. (1968) Physics Fluids 11, 1115.

SCHMIDT, G. (1966) Physics of High Temperature Plasmas, Academic Press, New York, 16.

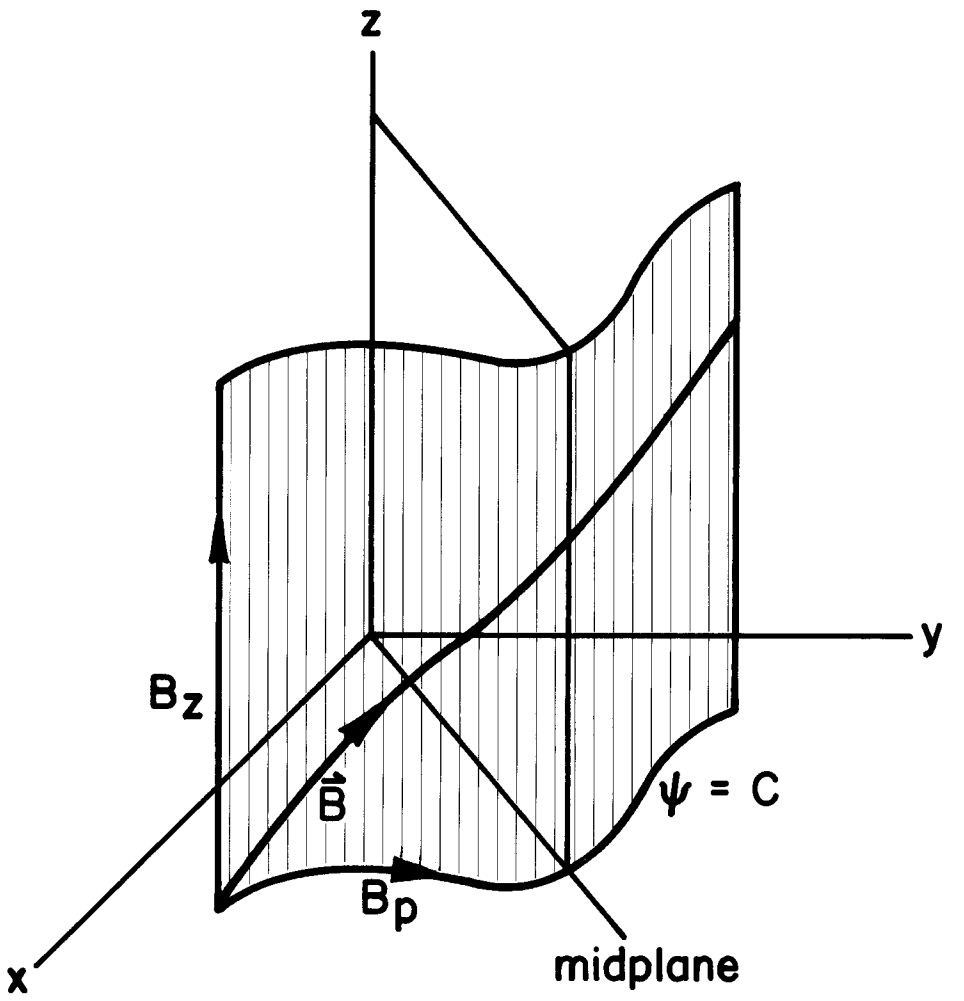

Fig. 1

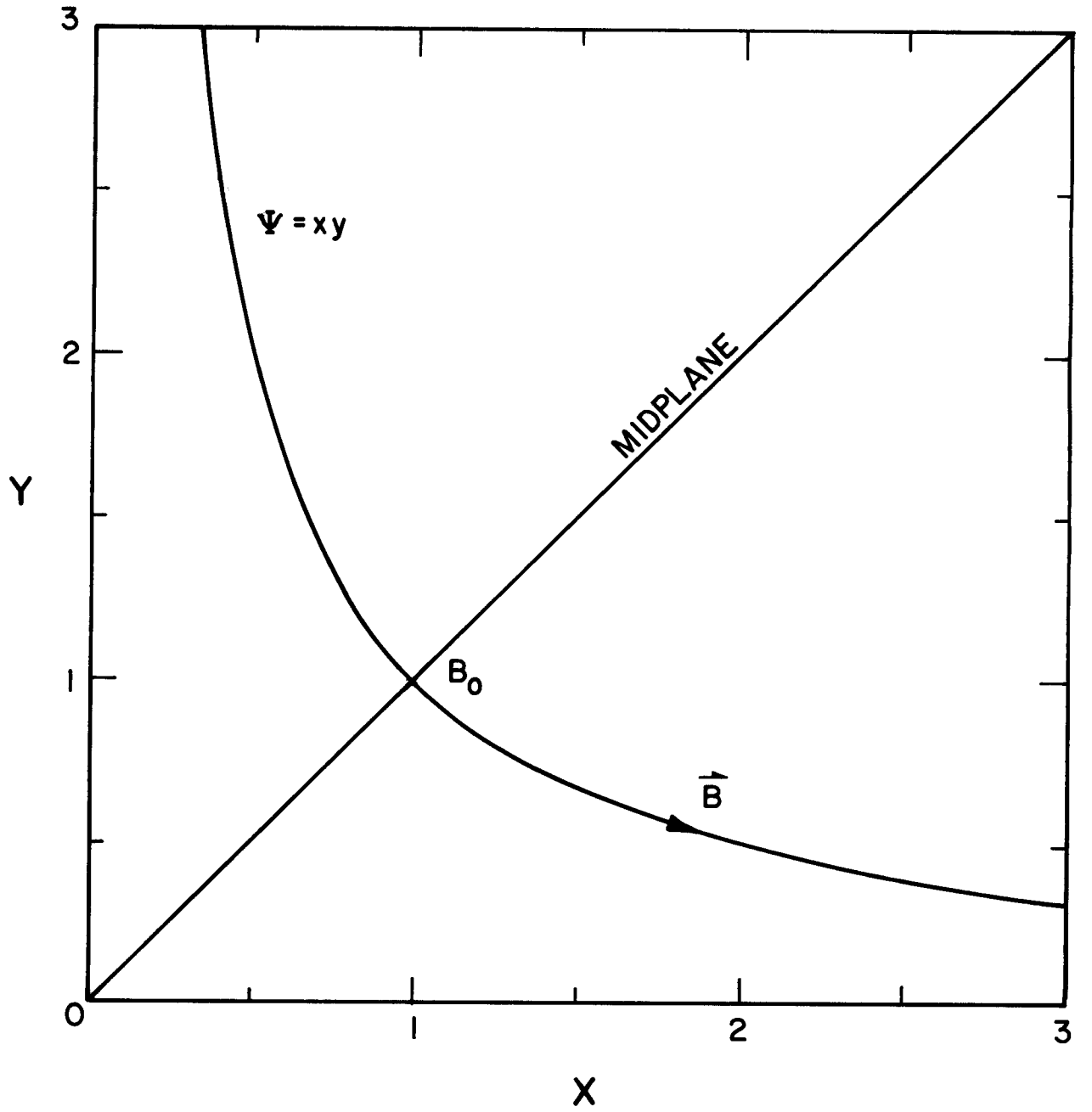

Fig. 2

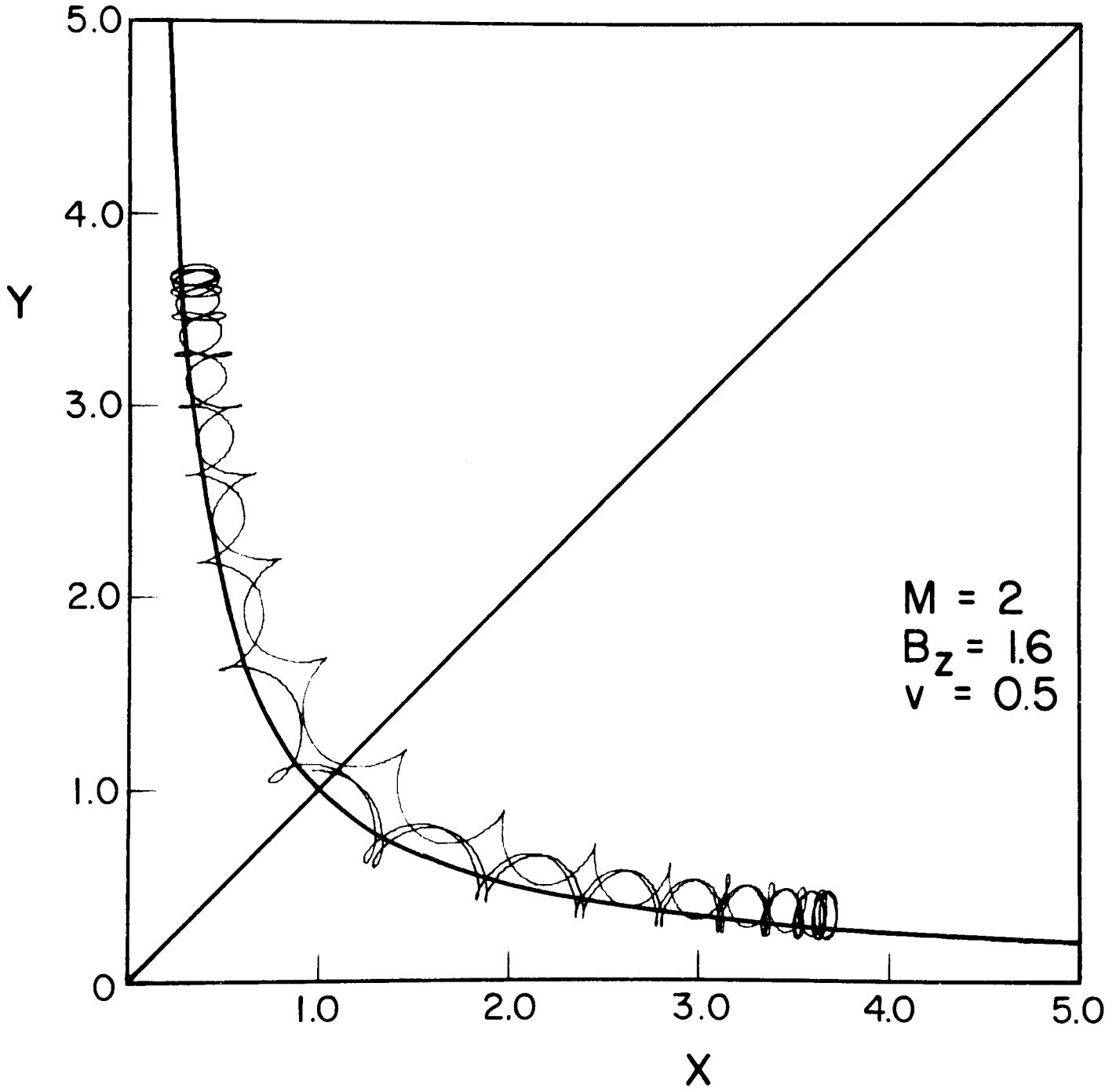

Figure 4

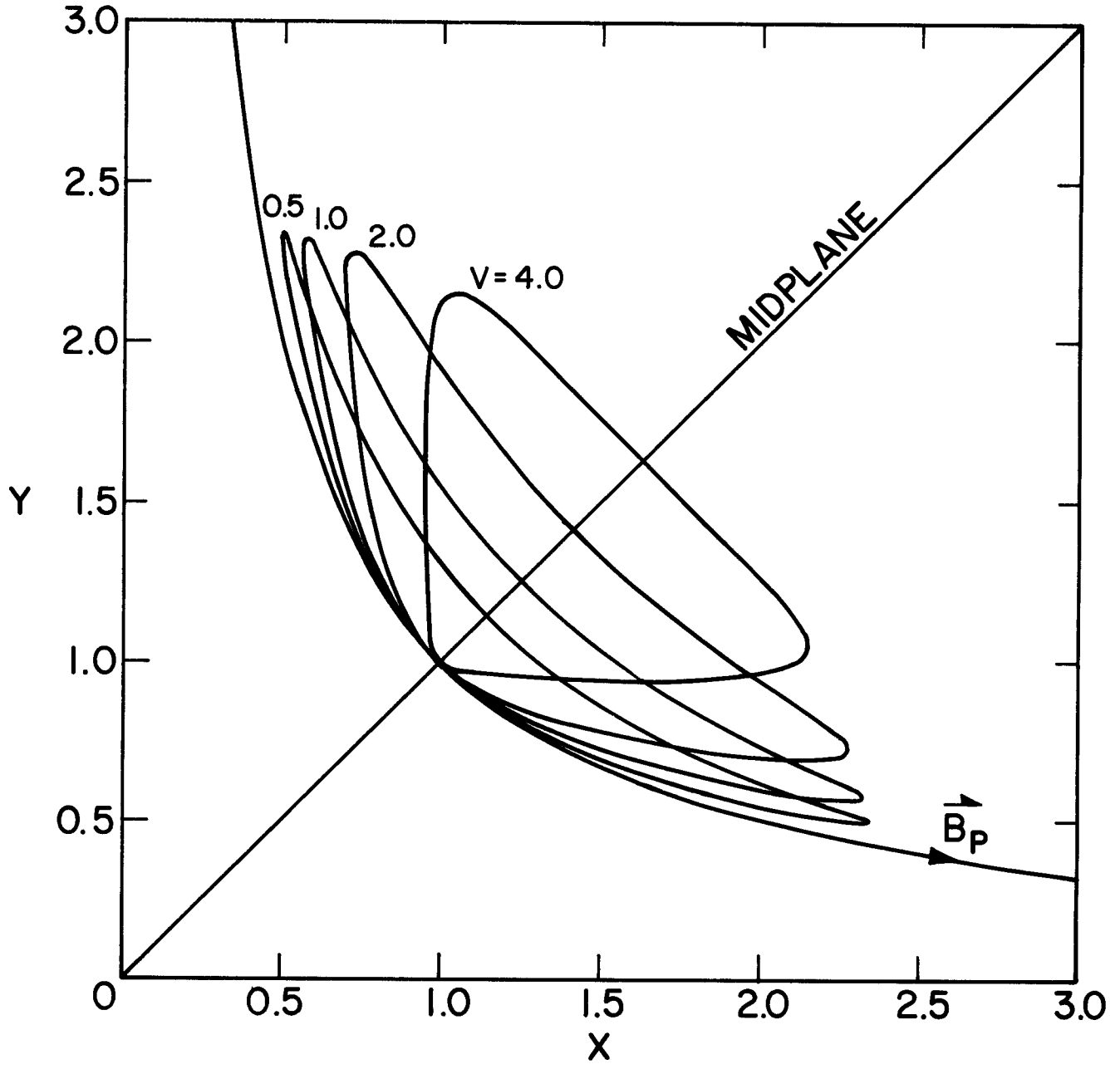

Fig. 5

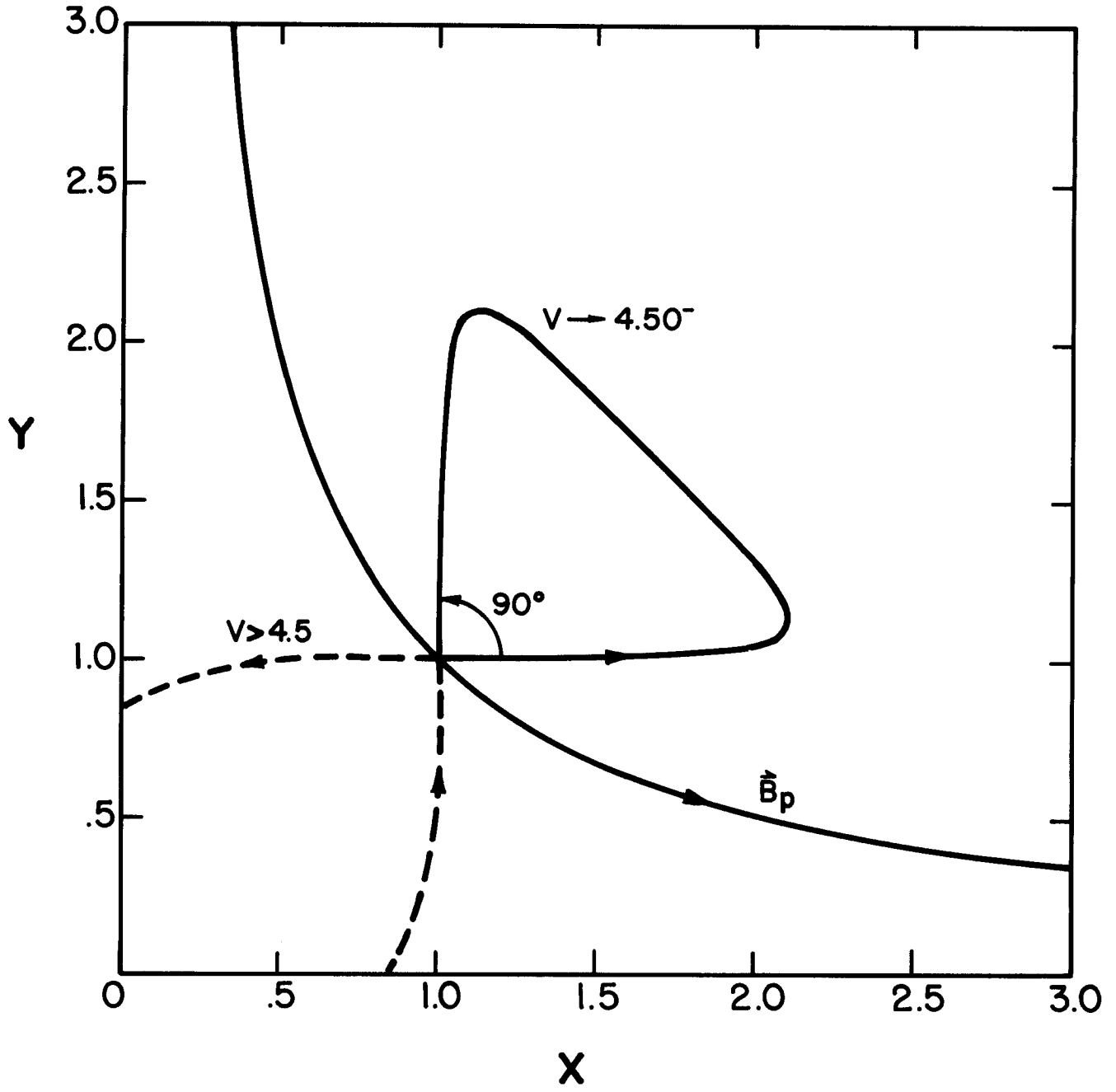

Fig. 6

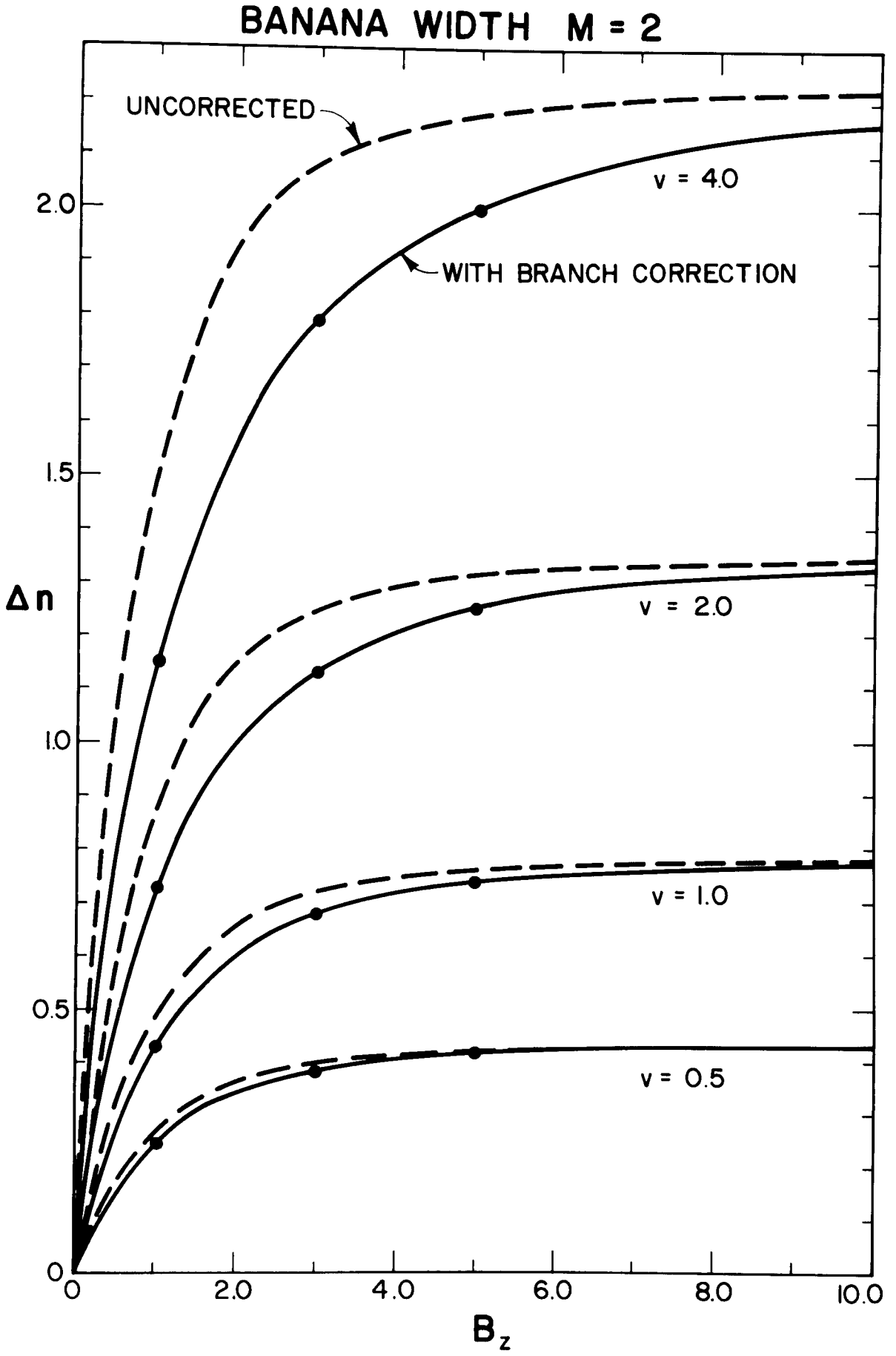
BANANA WIDTH M = 2
UNCORRECTED
WITH BRANCH CORRECTION
v = 4.0
v = 2.0
v = 1.0
v = 0.5
Δn
B_z
0
0.5
1.0
1.5
2.0
2.0
4.0
6.0
8.0
10.0

Figure 7

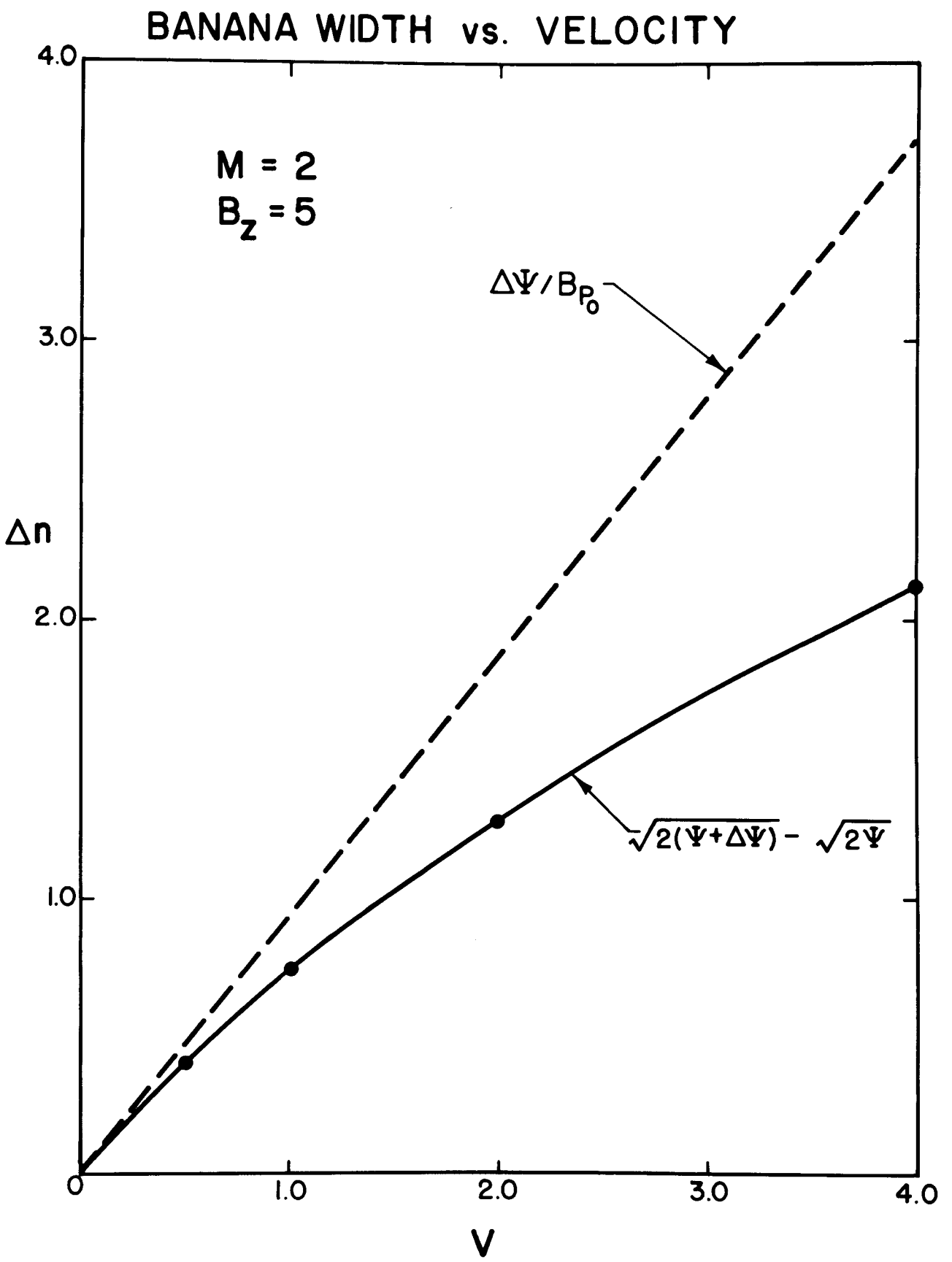
BANANA WIDTH vs. VELOCITY
M = 2
$B_z = 5$
$\Delta\Psi / B_{P_0}$
$\sqrt{2(\Psi+\Delta\Psi)} - \sqrt{2\Psi}$
Δn
V
0
1.0
2.0
3.0
4.0

Figure 8

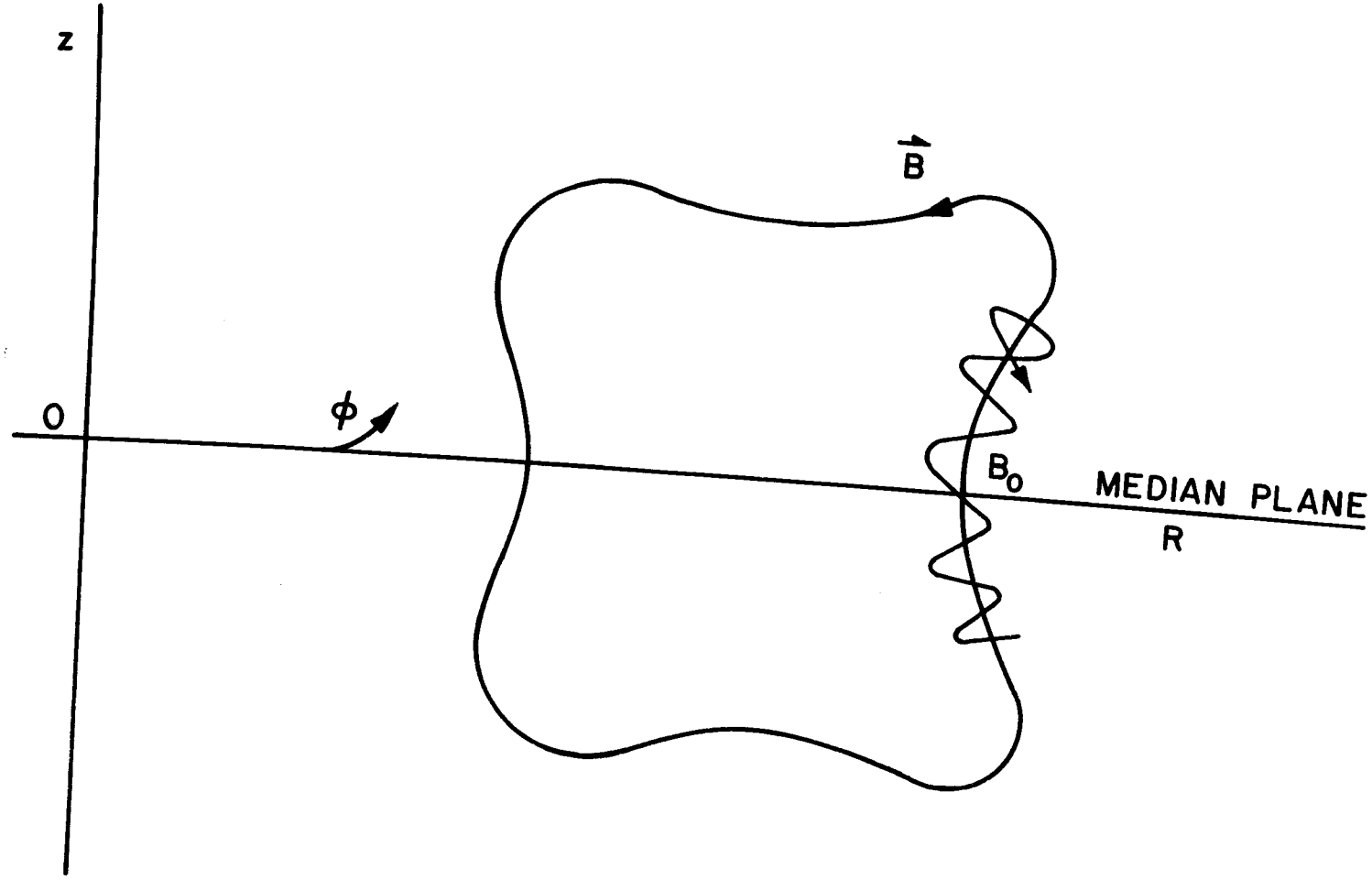

Fig. 9